

MODELING AND VALIDATION OF DAMPED PLEXIGLAS WINDOWS FOR NOISE CONTROL

Ralph D. Buehrle*, Gary P. Gibbs*, Jacob Klos*, and Marina Mazur†
NASA Langley Research Center
Hampton, Virginia 23681

Abstract

Windows are a significant path for structure-borne and air-borne noise transmission in general aviation aircraft. In this paper, numerical and experimental results are used to evaluate damped plexiglas windows for the reduction of structure-borne and air-borne noise transmitted into the interior of an aircraft. In contrast to conventional homogeneous windows, the damped plexiglas windows were fabricated using two or three layers of plexiglas with transparent viscoelastic damping material sandwiched between the layers. Transmission loss and radiated sound power measurements were used to compare different layouts of the damped plexiglas windows with uniform windows of the same nominal thickness. This vibro-acoustic test data was also used for the verification and validation of finite element and boundary element models of the damped plexiglas windows. Numerical models are presented for the prediction of radiated sound power for a point force excitation and transmission loss for diffuse acoustic excitation. Radiated sound power and transmission loss predictions are in good agreement with experimental data. Once validated, the numerical models were used to perform a parametric study to determine the optimum configuration of the damped plexiglas windows for reducing the radiated sound power for a point force excitation.

Introduction

Laminated glass has been shown to provide benefits for noise reduction in automotive and architectural applications.¹⁻⁴ Recent experimental work by Gibbs et. al.⁵ shows the potential benefits of damped plexiglas windows based on comparisons of transmission loss and radiated sound power. The damped plexiglas windows were evaluated as replacements for conventional solid aircraft windows to reduce the structure-borne and air-borne noise transmitted into the

interior of general aviation aircraft. The damped plexiglas windows were fabricated using two or three layers of plexiglas with transparent viscoelastic damping material sandwiched between the layers as shown in Figure 1. For windows that were nominally ¼" thick, reductions in the radiated sound power as large as 3.7 dB over a 1000 Hz bandwidth were shown experimentally when comparing damped and uniform windows. An increase in transmission loss of up to 4.5 dB over a 50 to 4000Hz frequency range was also shown.

This work extends the plexiglas window study⁵ to include finite element and boundary element modeling of the windows. Vibro-acoustic predictions were compared with vibration and acoustic response measurements for the windows installed in the NASA Langley Structural Acoustic Loads and Transmission (SALT) Facility.⁶ Good agreement between measurement and predictions were obtained. Comparisons between the numerical and experimental data validate the numerical modeling approach. Using the validated numerical models, a parametric study was used to examine the optimum layout of the damped plexiglas windows. The test facility, hardware, vibro-acoustic tests, and numerical models are described.

Test Facility

The Structural Acoustic Loads and Transmission (SALT) Facility⁶ located at the NASA Langley Research Center is shown in Figure 2. The SALT facility consists of an anechoic chamber, a reverberation chamber, and a shared transmission loss (TL) window. The anechoic chamber has a volume of 11,900 cubic feet (337 cubic meters). Interior dimensions of the anechoic chamber, measured from wedge tip to wedge tip, are 15 feet (4.57 meters) in height, 25 feet (7.65 meters) in width, and 32 feet (9.63 meters) in length. The reverberation chamber has dimensions of 14.8 feet (4.5 meters) in height, 21.3 feet (6.5 meters) in width, and 31.2 feet (9.5 meters) in length for a volume of 9,817 cubic feet (278 cubic meters). A shared TL window accommodates test structures of up to 54- by 54-inches (1.41- by 1.41-meters).

*Aerospace Engineer, Structural Acoustics Branch

†Cooperative Education Student, Purdue University

This material is declared a work of the U.S. Government and is not subject to copyright protection in the United States.

Hardware Description

A plexiglas window is shown installed in the SALT Facility in Figure 3. The SALT facility was setup as a transmission loss suite. A 48- by 24-inch plexiglas window was clamped between two 0.75-inch thick aluminum frames to approximate a fixed boundary condition. After mounting in the frame, the exposed portion of the plexiglas window measured 37.75- by 15.25-inches. The frame assembly was installed in a 3-inch thick fixture composed of medium density fiberboard, which was mounted in the transmission loss (TL) window.

Table 1. Nominally ¼ -Inch Test Windows

Window Configuration	Overall Thickness (inch)	Weight of Exposed Panel (lbs)
216	0.216	5.38
114,2,114	0.230	5.72
175,2,60	0.237	5.90
30,2,175,2,30	0.239	5.94
60,2,114,2,60	0.238	5.91

The numerical studies will focus on a set of nominally ¼ -inch thick windows. This set consists of a uniform window and four different layouts of damped plexiglas windows. Table 1 provides a list of the layouts for the windows. The thickness dimensions are in thousandths of an inch. For example, the 175,2,60 window has a 0.175-inch thick plexiglas layer, a 0.002-inch thick viscoelastic layer, and a 0.060-inch thick plexiglas layer. All damped window test configurations used a .002-inch thick 3M™ viscoelastic damping polymer (Product No. 112P02). Due to the thickness of the available plexiglas sheets, overall window thickness and corresponding window weight varied by approximately ten percent. The weight estimates are based on the exposed portion of the window (37.75- by 15.25-inches) and manufacturer provided density values. For this study, the windows were all manufactured flat for ease of fabrication and testing.

Vibro-Acoustic Tests

Measurements of the radiated sound power and transmission loss of the damped and undamped plexiglas windows were made by Gibbs et.al.⁵ A brief summary of the setup and results are provided below.

Radiated Sound Power

A plexiglas window was mounted in the TL window of the SALT facility and excited with psuedo random excitation by a shaker. The spatial intensity was measured⁷ with two-microphone intensity probes and the data was integrated over the measurement surface to obtain the radiated sound power. Figure 4 shows the results for several of the tested ¼-inch windows. The damped panels are shown to reduce the radiated sound power by up to 8 dB at some of the lower resonance frequencies and up to 3.7 dB over the 1000Hz bandwidth.

Transmission Loss

The SALT facility was setup as a transmission loss suite with the reverberation chamber on the source side of the window and the anechoic chamber on the receiver side. The reverberation room was driven with four speakers, each directed into a corner, to produce a diffuse acoustic excitation of the window. The transmission loss was found from measurements of the incident and transmitted sound power.⁷

The transmission loss of the 216 window and the 60,2,114,2,60 window are shown in Figure 5. The damped window shows a significant increase in the transmission loss at the resonance dip (80 Hz) and in the mass controlled region. This results in a 4.5 dB increase in transmission loss over a 50 to 4000Hz frequency range. For a homogeneous panel,⁸ the most significant improvement due to the addition of damping is expected at the lower resonant frequencies and above the coincident frequency. For the nominally ¼-inch thick plexiglas window the coincident frequency is approximately 6 kHz. As shown in figure 5, an increase in transmission loss of 6 dB is observed at and above coincidence, and at resonance.

Vibroacoustic Test Summary

The addition of a constrained viscoelastic damping layer provided a significant improvement in acoustic performance for the ¼-inch thick windows.⁵ The 60,2,114,2,60 window resulted in the best acoustical performance of the windows tested. However, the question of the optimum layup remained. It was desirable to develop and validate methods to predict the observed change in radiated sound power and transmission loss due to the incorporation of constrained layer damping in the plexiglas windows. This led to the numerical studies described in the remaining sections.

Numerical Models

Finite Element Model

MSC.Nastran 2001 was used for the finite element analyses. The viscoelastic layer was modeled with eight node solid elements with isotropic material properties. Plate (CQUAD4) and solid elements (CHEXA) were evaluated for the plexiglas base and constraining layers. Comparisons of the models and a discussion of required mesh will be provided in the results. Isotropic material properties were assumed for the plexiglas.

The material properties provided by the manufacturer for the plexiglas and viscoelastic damping material are listed in Table 2. Estimates of the damping properties of the plexiglas were based on comparisons with experimental results for the uniform window. The loss factor for both materials was entered as structural element damping (GE) on the material card of the finite element model. The viscoelastic damping material has frequency and temperature dependent properties. An ambient temperature of 20 degrees Celsius was assumed.

Table 2. Material Properties

Material	Poisson Ratio	Density lb-s ² /in ⁴	Shear Modulus psi	Loss Factor
Plexiglas	0.35	1.12e-4	246000	.07
Viscoelastic (100 Hz)	0.49	9.36e-5	362	1
Viscoelastic (300 Hz)	0.49	9.36e-5	725	.85
Viscoelastic (500 Hz)	0.49	9.36e-5	1015	.7
Viscoelastic (1000 Hz)	0.49	9.36e-5	1305	.6

A modal frequency response solution that included 200 modes, up to a frequency of over 4000 Hz, was used to predict the response to unit force excitation over the 60 to 1000 Hz range. As noted previously, the viscoelastic material had frequency dependent material properties. The modal frequency response solution does not allow for frequency dependent material properties, so predictions are based on constant viscoelastic material properties corresponding to the values at 100Hz. Incorporation of frequency dependent material properties requires the direct frequency response solution but this significantly increases computation time. As will be shown in the results section, the modal solution provided predictions

consistent with the measured results. For each of the window layups, surface velocities were predicted for a given excitation and used as boundary condition input to the boundary element model.

Boundary Element Model

The boundary element model was developed in COMET/Acoustics. A grid of 39 elements along the length by 16 elements along the width was used to obtain adequate spatial resolution of the structural mode shapes through 1000 Hertz. A symmetric boundary was used to simulate the acoustic radiation of the baffled window into the anechoic chamber. The direct exterior boundary element analysis was used to predict the radiated sound power from imposed surface velocity data. Surface velocity data was based on finite element analyses with point force excitation and also the diffuse acoustic excitation. In order to evaluate the numerical data, the finite element velocity predictions were first interpolated to the reduced mesh size of the boundary element model and then analyzed.

Diffuse Acoustic Excitation Model

The finite element models of the 216 window and the 60,2,114,2,60 window were used to predict the change in the sound power transmission loss due to the addition of constrained layer damping. To use the finite element models to predict the transmission loss, a simulation of the excitation mechanism present in the experiment is needed.

A diffuse acoustic excitation of the finite element models was developed based on plane wave propagation. A large number, N , of plane waves having random angles of incidence, random magnitudes, and random temporal phase angles were summed together to simulate a diffuse field excitation. A plane wave incident on the surface of a window at angles θ_n and ψ_n is shown in Figure 7. The angles θ_n and ψ_n are uniformly distributed random numbers on the intervals $[0,\pi]$ and $[0,2\pi]$ respectively and represent the angles of propagation in spherical coordinates. The n^{th} plane wave has a magnitude of $P_n \cos(\theta_n)$, where P_n is a uniformly distributed random number on the interval $[0,1]$. Thus the steady state pressure can be described in space and time by the equation

$$P_n(x, y, z, t) = P_n \cos(\theta_n) e^{-ik_x x} e^{-ik_y y} e^{-ik_z z} e^{i(\omega t + \phi_n)} \quad (1)$$

where ω is the angular frequency, ϕ_n is a random temporal phase angle uniformly distributed on the

interval of $[0, 2\pi]$, and k_x , k_y and k_z are the wavenumber in the x, y and z directions, respectively, found from

$$k_x = k \sin(\theta_n) \cos(\psi_n) \quad (2a)$$

$$k_y = k \sin(\theta_n) \sin(\psi_n) \quad (2b)$$

$$k_z = k \cos(\theta_n) \quad (2c)$$

where k is the wavenumber in air at a particular analysis frequency. The random temporal phase angle is introduced to prevent the N plane waves from having the same phase angle at the origin. A weighting function of $\cos(\theta_n)$ is included in the pressure magnitude to correct for the probability distribution of incident plane waves likely present in the experimental excitation.⁹ The random variables θ_n , ψ_n , P_n and ϕ_n are unique for each of the N plane waves. Assuming steady state simple harmonic motion and a nearly rigid boundary condition at the surface of the window, the spatial pressure distribution exciting the window can be approximated by

$$\hat{P}_n(x, y, z, \omega) = 2P_n \cos(\theta_n) e^{i\phi_n} e^{-ik_x x} e^{-ik_y y} e^{-ik_z z} \quad (3a)$$

or

$$\hat{P}_n(x, y, z, \omega) = 2P_n \cos(\theta_n) e^{i(\phi_n - k_x x - k_y y - k_z z)} \quad (3b)$$

where x , y and z are evaluated on the surface and k_x , k_y and k_z are evaluated at a particular angular frequency ω . The pressure acting on the surface of each element, e , in the finite element model, due to the N plane waves, was computed using the x, y and z coordinates of the element center x_e , y_e and z_e . The total pressure at the center of each element, P_e , due to N incident plane waves is

$$\hat{P}_e(\omega) = \sum_{n=1}^N 2P_n \cos(\theta_n) e^{i(\phi_n + k_x x_e + k_y y_e + k_z z_e)} \quad (4)$$

where N is the number of plane waves used to approximate the diffuse field. This pressure distribution acting on the surface elements of the finite element model was used as an excitation. The velocity response of the finite element model was predicted due to the pressure excitation. The predicted velocities were imported into the boundary element model of the window and the transmitted sound power, Π_t , was predicted.

To compute transmission loss, the ratio of the incident to transmitted sound power is needed.

The incident sound power is computed from the intensity vector of each of the N plane waves. The intensity vector, \vec{I}_n , of the n^{th} plane wave is

$$\vec{I}_n = -\frac{[P_n \cos(\theta_n)]^2}{\rho c} [\sin(\theta_n) \cos(\psi_n) \vec{i} + \sin(\theta_n) \sin(\psi_n) \vec{j} + \cos(\theta_n) \vec{k}] \quad (5)$$

The intensity normal to the surface of the window is the z component of the intensity vector (Figure 2). The sound power incident on a window of area A due to the n^{th} plane wave is

$$\Pi_{i,n} = A \cos(\theta_n) \frac{[P_n \cos(\theta_n)]^2}{\rho c} \quad (6)$$

The total incident sound power for all N plane waves is

$$\Pi_i = \sum_{n=1}^N \Pi_{i,n} \quad (7)$$

The transmitted sound power is computed as outlined above. The predicted transmission loss of the window is computed from the ratio of the incident and transmitted sound power

$$TL = 10 \log_{10} \left(\frac{\Pi_i}{\Pi_t} \right) \quad (8)$$

Results and Discussion

Finite Element Model

Concerns over stiffening effects associated with solid elements with high aspect ratios (length or width to thickness ratio) lead to a mesh refinement study. Mesh refinement for the solid (CHEXA) element model was based on comparison of a solid model with five elements through the thickness (60,2,114,2,60 window configuration) and plate models with uniform plexiglas material properties for all elements. A modal frequency response analysis for point force excitation from 60 to 1000 Hz was used for comparison of the various models. For this study, 200 modes were included in the modal frequency response solution, which accounts for modes with frequencies through 4000 Hz. A 38x15 mesh (approximately 1 inch square element) was used as the baseline. Figure 7 shows the results of predictions for three different meshes of the solid model. As can be seen, there was a stiffening

effect for the 38x15 mesh but the results for the 76x30 and 152x60 solid element mesh did not change significantly. The predictions for the 76x30 solid element mesh were also in excellent agreement with the plate model results. Therefore, a mesh of 76x30 solid elements was determined to be sufficient.

In earlier work on the finite element analysis of damped structures,^{10,11} the viscoelastic layer was modeled with solid elements but the base and constraining layer were modeled with plate elements. Plate elements offer the advantage of a reduced number of degrees of freedom if the plates are defined on the surface of the solid elements with offsets used to account for the location of the mid-plane. A model using plate elements for the base and constraining layers for a 175,2,60 layup with uniform plexiglas properties was compared to a uniform plate model. A 76x30 element mesh was used. Figure 8 shows the results of a modal frequency response analysis. The plate-solid-plate model was consistent at lower frequencies but had a softening effect in the higher frequencies. This softening effect was not present in the solid models shown in Figure 7. Therefore, a solid model was used for all layers in subsequent analyses.

Radiated Sound Power Prediction

The measured and predicted sound power for a uniform plexiglas window and a damped plexiglas window are shown in Figures 9 and 10, respectively. Measured and predicted results are in good agreement. Discrepancies at the first resonant frequency are associated with a coupling of a window mode and a mode of the supporting fiberboard test fixture. The test fixture is not included in the finite element model and therefore its dynamic effects are not captured in the predicted results. Above 500 Hz, predictions have higher damping than the experiment but consistent trends in magnitude are observed. The predicted sound power for several damped plexiglas window layups are shown in Figure 11. Reductions in the radiated sound power of as much as 7 dB at some of the lower frequencies and 3.3 dB over the 1kHz bandwidth are demonstrated. These predicted reductions are consistent with experimental results shown previously in Figure 4.

Parametric Study

A parametric study was performed to examine the optimum placement of viscoelastic damping material within a nominally 0.25" thick plexiglas

window. Utilizing test verified finite element models, windows with two and three plexiglas layers with viscoelastic damping material sandwiched between each layer were analyzed. The total amount of viscoelastic material was held constant for all of the window layups. The two layer windows used a single .004" thick viscoelastic layer while the three layer windows had two .002" thick viscoelastic layers. Figure 12 shows the results of the parametric study. For a symmetric three-layer plexiglas window, the radiated sound power decreased as the center plexiglas layer thickness decreased and the optimum design converged to a window with two equal thickness plexiglas layers. Results for the two layer designs also showed the greatest reductions were obtained for two plexiglas layers of equal thickness with the viscoelastic material at the mid-plane. This is consistent with published¹² panel damping design recommendations when the base and constraining layers are made of the same material.

TL Prediction

The 216 and the 60,2,114,2,60 window were studied. The measured change in the transmission loss caused by the addition of the constrained layer damping was computed from the measured transmission loss data shown in Figure 5. The measured change in transmission loss is shown in Figure 13, red line. The change in transmission loss was most significant at the first resonance of the panel where an increase of 6 dB was observed. In the mass controlled region, an increase of 1 to 2 dB was observed in the transmission loss. Using the combined finite element, boundary element and diffuse acoustic field models, predictions of the transmission loss of the 216 and the 60,2,114,2,60 plexiglas windows were made. The predicted change in transmission loss was computed (Figure 13, green curve). There is good agreement between the measured and predicted change in transmission loss caused by the addition of the damping layer. In general, the predicted change in transmission loss is within 0.5 dB of the measurement (Figure 13). The finite element model of the panel incorporating the modal frequency response solution was used. The damping loss factor and shear stiffness of the viscoelastic damping layer were assumed to be constant with respect to frequency. However, the properties of the viscoelastic damping layer used in the experiment varied with respect to frequency. The errors observed when comparing the measured and predicted change in transmission loss are likely

due to difficulty estimating the viscoelastic properties of the damping layer and variation of the viscoelastic properties with frequency.

Summary and Conclusions

Numerical modeling of plexiglas windows showed good agreement with experimental data. The 60,2,114,2,60 window resulted in the best acoustical performance of the windows tested. The numerical models were used to determine the optimal damped plexiglas panel configuration. Based on a parametric study of two and three layer plexiglas windows with equal amounts of viscoelastic material, the optimum design converged to a window with two equal thickness plexiglas layers. These results show that it is most advantageous to place all of the damping material at the mid-plane where the shear strains are the largest. The modeling approach has been validated and can be used to evaluate other design configurations. Predicted reductions in the radiated sound power of as much as 7 dB at some of the lower frequencies and 3.3 dB over the 1kHz bandwidth demonstrate the potential of damped windows for noise control applications.

The change in transmission loss caused by the constrained layer damping was predicted using a simulated diffuse acoustic excitation of the finite element model. There was good agreement between the measured and predicted change in transmission loss caused by incorporation of the viscoelastic damping layer in the window. This method can be used to study sound transmission properties of windows and other structures that incorporate constrained layer damping.

Reference:

1. Pyper, J., "Laminated Glass Provides Noise Barrier Benefits in Automobile and Architectural Applications," *Sound and Vibration*, August 2001, pp. 10-16.
2. Freeman, G. E., and Esposito, R. A., "Glazing for Vehicle Cabin Sound Reduction," *Proceedings of Inter-noise 2002*, Detroit, Michigan.
3. Lu, J., "Passenger Vehicle Interior Noise Reduction by Laminated Side Glass," *Proceedings of Inter-noise 2002*, Detroit, Michigan.
4. Lu, J., "Designing PVB Interlayer for Laminated Glass with Enhance Sound Reduction," *Proceedings of Inter-noise 2002*, Detroit, Michigan.
5. Gibbs G., R. Buehrle, J. Klos and S. Brown, 2002, "Noise Transmission Characteristics of Damped Plexiglas Windows", AIAA 2002-2416, *Proceedings of the 8th AIAA/CEAS Aeroacoustics Conference*, Breckenridge, Colorado, June 17-19,2002.
6. Grosveld, F. W., "Calibration of the Structural Acoustic Loads and Transmission Facility at NASA Langley Research Center," *Proceedings of the Inter-noise 99*, Fort Lauderdale, Florida.
7. Klos, J., and S. A. Brown, 2002, "Automated transmission loss measurement in the Structural Acoustic Loads and Transmission facility at NASA Langley Research Center", *Proceedings of Inter-noise 2002*, Detroit, Michigan.
8. Lord, H. W., Gatley, W. S., and Evensen, H. A., *Noise Control For Engineers*, McGraw-Hill, Inc., New York, 1980, pp.243
9. Fahy, F., *Sound and Structural Vibration: Radiation, Transmission and Response*, London: Academic Press, 1995.
10. Johnson, C.D., et.al., "Finite Element Design of Viscoelastically Damped Structures," *Proceedings of the AFWAL Vibration Damping Workshop*, 1984
11. Kluesener, M. F., "Results of Finite Element Analysis of Damped Structures," *Proceedings of the AFWAL Vibration Damping Workshop*, 1984
12. Ungar, E. E., *Damping of Panels*, Chapter 6, *Noise and Vibration Control*, Edited by Leo L. Beranek, McGraw Hill, Inc., 1971

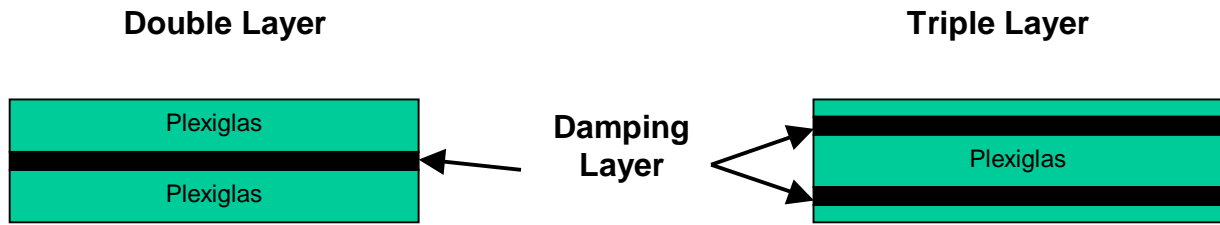


Figure 1. Damped plexiglas window configurations

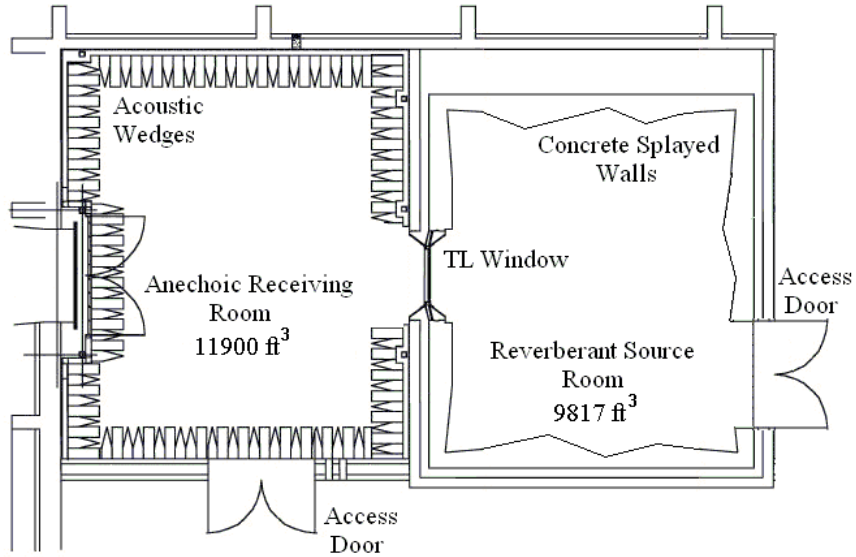


Figure 2. Schematic of SALT Facility.

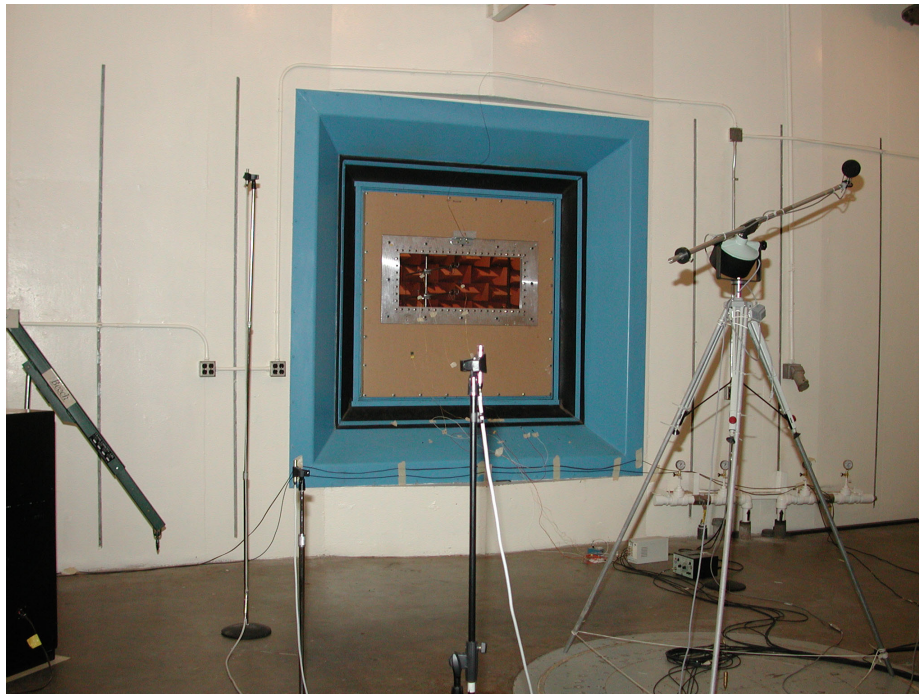


Figure 3. Plexiglas window installed in SALT TL window, view from reverberation chamber.

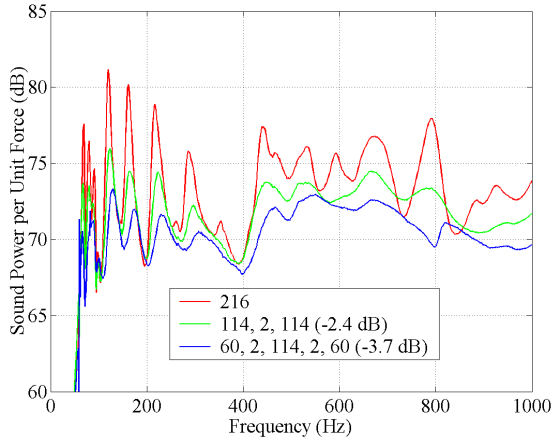


Figure 4. Measured radiated sound power for nominally 1/4-inch thick windows installed in SALT.

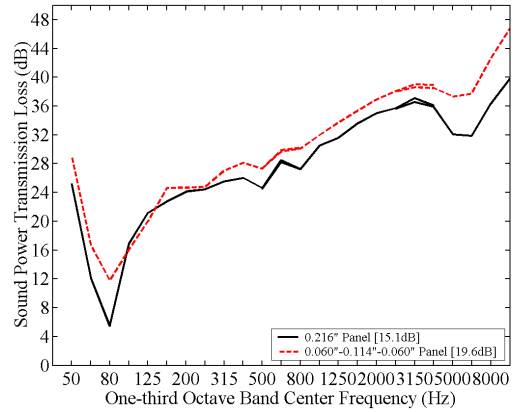


Figure 5. Measured transmission loss of the undamped “—” and damped “- - -” windows.

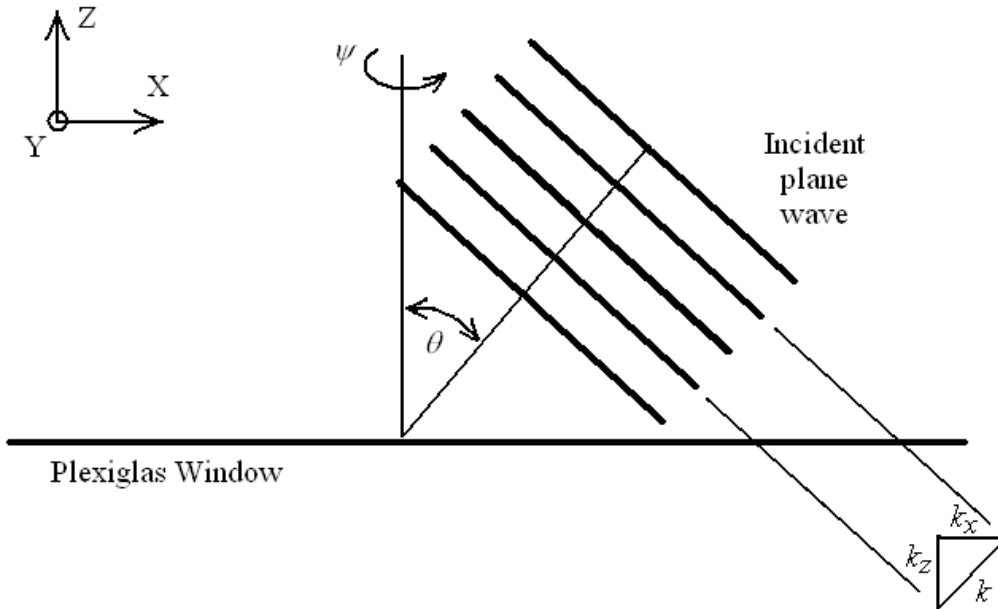


Figure 6: Plane wave incident on a Plexiglas window. The plane wave is shown propagating in the x-z plane, the y axis is into the page. The angle ψ represents a rotation of the heading of the plane wave about the z axis.

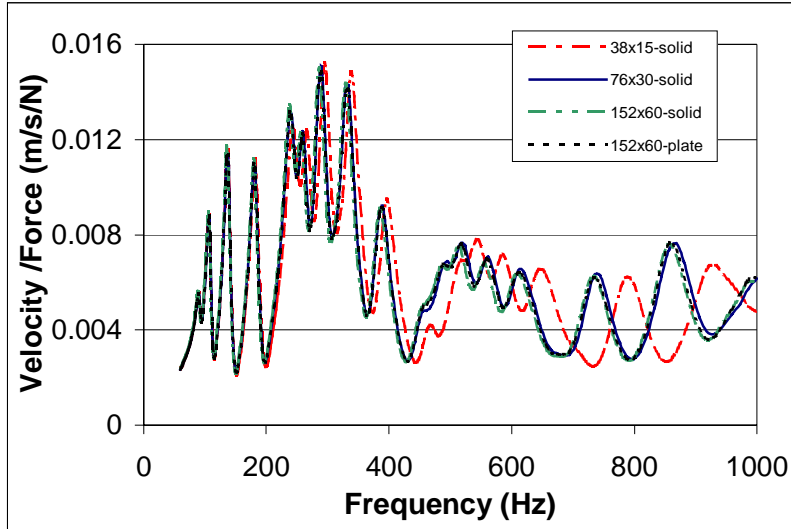


Figure 7. Drive point frequency response functions for FEM mesh refinement study.

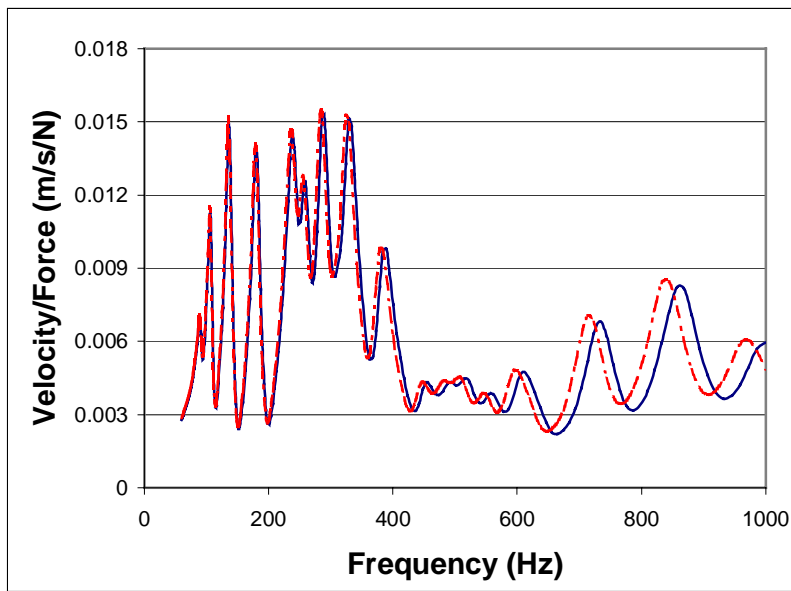


Figure 8. Drive point frequency response for uniform plate (solid) and plate-solid-plate (dashed) models.

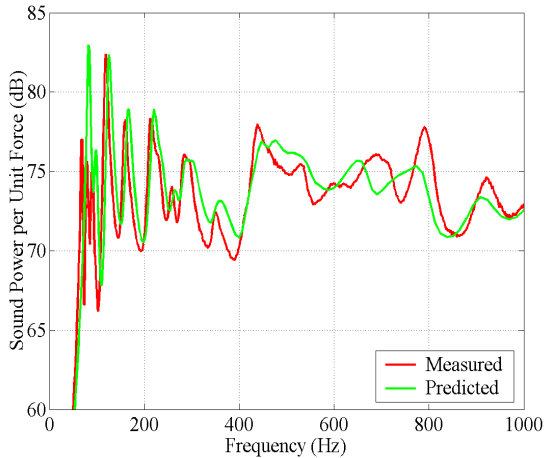


Figure 9. Measured and predicted radiated sound power for 216 panel.

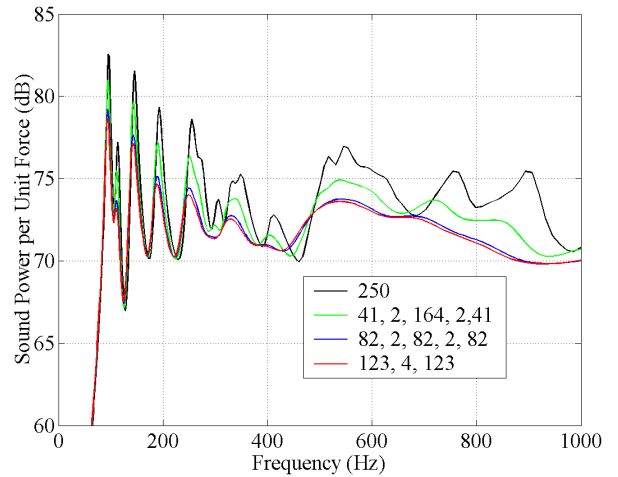


Figure 12. Results of parametric study showing the effect of window layout.

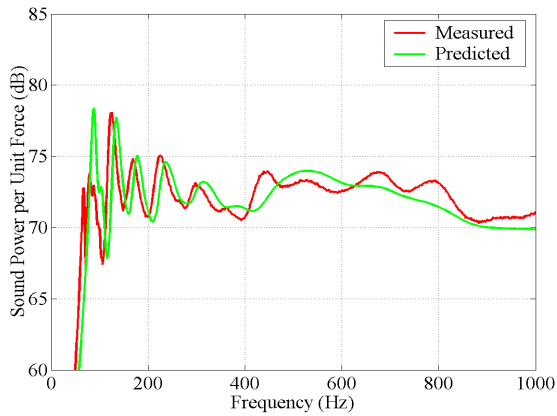


Figure 10. Measured and predicted radiated sound power for 114,2,114 panel.

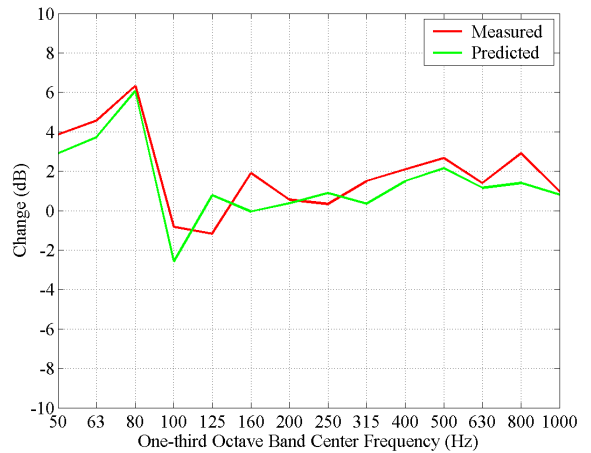


Figure 13. Comparison of the change in transmission loss due to the constrained layer damping.

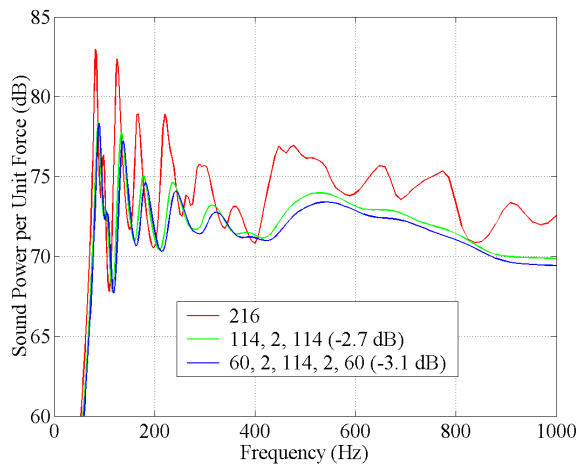


Figure 11. Predicted radiated sound power for point force excitation.